AGU ADVANCING EARTH AND SPACE SCIENCE

Geophysical Research Letters®

RESEARCH LETTER
10.1029/2021GL097190

Improving the Predictability of Two Types of ENSO by the Characteristics of Extratropical Precursors

Yu-heng Tseng[1], Jo-Hsu Huang[1], and Han-Ching Chen[2,3]

[1]Institute of Oceanography, National Taiwan University, Taipei, Taiwan, [2]Key Laboratory of Meteorological Disaster of Ministry of Education, Nanjing University of Information Science and Technology, Nanjing, China, [3]Department of Atmospheric Sciences, University of Hawai'i at Mānoa, Honolulu, HI, USA

Key Points:

- Both predictabilities of Central Pacific (CP)/Eastern Pacific (EP) El Niño-Southern Oscillation (ENSO) can be greatly enhanced by including the Pacific extratropical precursors
- The distinct roles of North and South Pacific precursors on the CP and EP ENSO, respectively, are clarified
- The stable/decreased predictability of CP/EP indices after 2000 confirms the recent enhanced NPO-relevant impacts

Supporting Information:

Supporting Information may be found in the online version of this article.

Correspondence to:

Y.-h. Tseng and H.-C. Chen,
tsengyh@ntu.edu.tw;
hanching@hawaii.edu

Citation:

Tseng, Y.-h., Huang, J.-H., & Chen, H.-C. (2022). Improving the predictability of two types of ENSO by the characteristics of extratropical precursors. *Geophysical Research Letters*, *49*, e2021GL097190. https://doi.org/10.1029/2021GL097190

Received 23 NOV 2021
Accepted 21 JAN 2022

Author Contributions:

Conceptualization: Yu-heng Tseng, Han-Ching Chen
Formal analysis: Jo-Hsu Huang
Methodology: Yu-heng Tseng, Han-Ching Chen
Writing – original draft: Yu-heng Tseng, Han-Ching Chen
Writing – review & editing: Yu-heng Tseng, Han-Ching Chen

Abstract The Central Pacific (CP) and Eastern Pacific (EP) types of El Niño-Southern Oscillation events are distinctly different in terms of their forming locations and mechanisms. Using an updated physical-base statistical forecast model, the forecast of CP indices has overall higher skills than that of EP indices due to the higher persistent forecast skill. At lead time beyond 6-month, the predictability of CP indices can be greatly enhanced by including the extratropical precursor from the North Pacific, confirming the ocean-atmosphere interaction associated with North Pacific Oscillation (NPO)/Victoria Mode (VM) evolution. The predictability of EP indices can be moderately enhanced by including the extratropical precursor from the south, resulting from the charging of the equatorial Pacific. We also find that the predictability of CP indices does not significantly decrease after 2000 while the predictability of EP indices drops dramatically, suggesting the strengthening impacts of NPO/VM on the CP-ENSO in the recent two decades.

Plain Language Summary The predictability of different types of El Niño-Southern Oscillation (ENSO) events can be significantly enhanced by including extratropical signals using a physical-base statistical forecast model. At a lead time longer than 6-month, the predictability of Central Pacific ENSO can be greatly enhanced by including the extratropical signal from the North Pacific, confirming a well-known ocean-atmosphere interaction process proposed earlier. The predictability of Eastern Pacific ENSO can be moderately enhanced by including the extratropical precursor from the south, resulting from the charging of the equatorial Pacific. We also find that the predictability of CP indices does not significantly decrease after 2000 while the predictability of EP indices drops dramatically, suggesting the enhanced north hemispheric impacts in the recent two decades.

1. Introduction

El Niño-Southern Oscillation (ENSO) prediction has the most severe forecast bottleneck. A recent study has suggested that the ENSO prediction can be greatly enhanced using extratropical precursors in the Pacific (H.-C. Chen et al., 2020). By combining tropical preconditions/ocean-atmosphere interaction with extratropical precursors, the ENSO prediction skill can be significantly enhanced beyond the spring predictability barrier (SPB), resulting mainly from the long lead-time of the extratropical-tropical, ocean-atmosphere interaction processes.

Nevertheless, the predictability of the two types of ENSO, the eastern Pacific (EP) and central Pacific (CP) types, classified in terms of the zonal displacement of warm Sea Surface Temperature (SST) anomalies, remains very challenging due to the uncertainties associated with different ENSO dynamics (Ren et al., 2019). The causes of CP-ENSO have been shown distinctly different from those of the EP types (e.g., Kao & Yu, 2009; Kim et al., 2009), thus leading to different prediction skills. Recent studies have assessed the model performances in predicting the two ENSO types (e.g., Ren et al., 2016, 2019; Yang & Jiang, 2014; Zhu et al., 2015). These studies show that the EP-ENSO has a relatively higher prediction skill than the CP-ENSO, even though the latter tends to persist longer than the former in terms of the Niño indices (Kim et al., 2009; Ren et al., 2019).

However, Ren et al. (2019) argued that the extratropical precursors might have limited contributions to improve the prediction skills of these two ENSO types at specific initial months and leads. They found that most signals within these precursors have already transferred into the variation of the two indices in their benchmark model based on the equatorial Pacific heat content and zonal wind stress. Only the northern tropical Atlantic SST precursor can provide additional prediction skill score for both types of ENSO beyond the SPB. This raises some doubts about the role of extratropical impacts on the ENSO prediction.

Since many prediction models lose skills in predicting the El Niño type after one season (e.g., Hendon et al., 2009; Tao et al., 2020), especially for the CP-El Niño. The characteristics of these two types of ENSO also make their forecast more challenging due to their distinct dynamics, such as the eastward propagation property or onset mechanisms (C. Chen et al., 2017; Timmermann et al., 2018; Yu & Fang, 2018). This study revises the physical-base statistical forecast model based on H.-C. Chen et al. (2020) and Ren et al. (2019) to improve the predictability of CP and EP-ENSO. Particularly, this is the first study to clarify the key roles of extratropical precursors from the northern and southern Pacific affecting the CP-ENSO and EP-ENSO, respectively, from the predictability viewpoint. The predictability of CP-ENSO can be significantly enhanced, even superior to that of EP-ENSO. Physical processes leading to the improved prediction of these two ENSO types can be well explained based on their evolution pathways.

2. Data and Methods

2.1. Observation Data and ENSO Definition

The observed SST used here is the monthly 2° × 2° NOAA Extended Reconstructed Sea Surface Temperature version 5 (ERSSTv5; Huang et al., 2017). The 20°C isotherm depth (D20) is calculated from the pentad global ocean data assimilation system (GODAS) on a 1/3° latitude × 1.0° longitude global grid (Behringer & Xue, 2004). The near-surface wind data (0.995-sigma level) and sea level pressure data come from the National Centers for Environmental Prediction and the National Center for Atmospheric Research (NCEP-NCAR) reanalysis project on a 2.5° × 2.5° horizontal grid resolution (Kalnay et al., 1996). All data range from 1980 to 2020, and the anomalies are based on the 30-year climatology of 1991–2020.

A simple way to represent the two types of ENSO is to use the typical Niño3, and Niño4 indices, calculated as SST anomalies (SSTA) averaged over the Niño3 (5°S–5°N, 150°–90°W) and Niño4 (5°S–5°N, 160°E–150°W) regions, respectively. However, the characteristics of these two ENSO types are not easily distinguishable (correlation reaches 0.74). Based on Ren and Jin (2011), we use the nearly orthogonal EP Niño index (N_{EP}) and the CP Niño index (N_{CP}) to represent the two types of ENSO in this study, respectively. N_{EP} and N_{CP} indices are defined as:

$$\begin{cases} N_{EP} = \text{Niño3} - \alpha \cdot \text{Niño4} \\ N_{CP} = \text{Niño4} - \alpha \cdot \text{Niño3}, \end{cases} \tag{1}$$

where $\alpha = 0.4$ when Niño3 multiplied by Niño4 is positive and $\alpha = 0$ otherwise. The correlation between N_{EP} and N_{CP} is reduced to 0.12. In this study, both typical and orthogonal ENSO indices are included for comparison. Other different indices of ENSO diversity, such as the EP-CP index method (Kao & Yu, 2009), the E and C indices (Takahashi et al., 2011), and the El Niño Modoki index (EMI; Ashok et al., 2007), are also examined (Figure S1 in Supporting Information S1). The results are unchanged and robust from the conclusions using the N_{EP} and N_{CP} indices regardless of the chosen indices (although the correlations are slightly different). A 3-month running mean is applied throughout our analysis to be consistent with the typical ENSO definition. All final comparisons between observations and forecast are made on a monthly timescale although daily NCEP-NCAR or pentad GODAS reanalysis data is used.

2.2. ENSO Prediction Model

The updated physical-base statistical forecast model, ENSO prediction model (EPM), is built as follows:

$$\text{EPM}(t+\varphi) = \frac{\sigma_O(m)}{\sigma_P(m)}[\beta_1(\varphi)\text{EP}_{\text{SST}}(t) + \beta_2(\varphi)\text{EP}_{\text{WWV}}(t) + \beta_3(\varphi)\text{EP}_{\text{OA}}(t) + \beta_4(\varphi)\text{EP}_{\text{EX}}(t)] \tag{2}$$

Four ENSO predictors are used, including the ENSO's SSTA index itself (EP_{SST}), the predictors according to the warm water volume (WWV) propagation in the central tropical pacific (EP_{WWV}), the ocean-atmosphere feedback (EP_{OA}), and the extratropical forcing term (EP_{EX}). EP_{SST} represents the SSTAs persistence measured by the predictand at the current time, which can improve the prediction skill in 1–3 months leading time (Ren et al., 2019). The eastward propagating WWV contribution (EP_{WWV}) is determined by the D20 anomalies at three different

longitudes (180°, 170°W, and 155°W) averaged between 2°S and 2°N at different time before and at the current time. The time-evolved propagating signals of WWV can be quantitatively represented by the combination of deepening or shallowing at these three locations. These longitudes and timings (days) are chosen based on the existing TAO array stations which can provide a more accurate forecast than the GODAS data if used (Tseng, Hu, et al., 2017). The ocean-atmosphere feedback (EP_{OA}) is estimated by the zonal surface wind anomalies over the equatorial central Pacific (180°–170°W, 2°S–2°N). The extratropical forcing term (EP_{EX}) is defined as follows:

$$EP_{EX} = (SLPA_{N1} - SLPA_{N2}) + (SLPA_{S2} - SLPA_{S1}), \quad (3)$$

where SLPA indicates the sea level pressure anomaly and the subscript N1 (165°–115°W, 50°–65°N), N2 (175°–120°W, 5°–30°N), S1 (180°–130°W, 20°–45°S), and S2 (180°–105°W, 50°–70°S) denote the four key regions associated with the ENSO evolution (green boxed from top to bottom in Figure 2). The EP_{WWV}, EP_{OA}, and EP_{EX} are calculated by the original daily/pentad data and then averaged to monthly data. Detailed definitions of these three terms can be found in Tseng, Hu, et al. (2017) and H.-C. Chen et al. (2020).

All predictors are standardized on their own before building the model. The regression coefficients (β_1, β_2, β_3, and β_4) are derived from the multivariate linear regression, which are the functions of forecast lead-time (φ). The monthly scaling function, $\frac{\sigma_O(m)}{\sigma_P(m)}$, is to adjust the seasonal variance of prediction to observations, where σ_O and σ_P are the standard deviations of SSTA for the observations and prediction, respectively, in different calendar months (m). This rescaling is used to calibrate the common biases of statistical model which cannot well predict ENSO magnitude. Eventually, the statistical EPM time series in different lead-month is built to predict the ENSO index and evaluate their hindcast skill. This revised EPM (updated from H.-C. Chen et al., 2020) has been well verified and it is one of the only three forecast models within the IRI/CPC ENSO plume which predict the occurrence of 2021–2022 La Niña in April 2021 (https://iri.columbia.edu/our-expertise/climate/forecasts/enso/2021-April-quick-look/).

3. Results

3.1. Characteristics of CP and EP Types of ENSO Evolution

The characteristics of the two types of ENSO can be distinguished by their spatial-temporal evolution. Figures 1a–1f show the lead-lag correlation between Niño3 (shading)/Niño4 (contours, positive is solid and negative is dashed) and the equatorial SST, D20 and zonal surface wind anomalies, respectively. The SSTA center of Niño3 (correlation >0.8) locates more eastward than that of Niño4, and is accompanied by similar zonal differences in D20 and zonal wind evolutions. However, the high correlation zones for the D20 (correlation >0.6) shift to an earlier time before the matured phase, confirming its potential role in the ENSO prediction regardless of ENSO types (Meinen & McPhaden, 2000). Particularly, both types of ENSO emerge from the central Pacific, where the interior transport of Subtropical Cell is strongest (H.-C. Chen et al., 2015) and the evident Kelvin wave propagation is initiated (Tseng, Hu, et al., 2017). These two processes control the main equatorial ocean predictor WWV and lead to the high correlations of D20 that can extend up to 6 months ahead in the central Pacific. Also, the correlations for all fields are higher for Niño3 than Niño4 in general, suggesting a closer connection of WWV with Niño3. This is consistent with previous studies reporting that EP ENSO is associated with stronger discharge/recharge processes than CP ENSO (e.g., Ren & Jin, 2013; Geng et al., 2020). However, we note that the characteristics of the two ENSO types are not easily distinguishable due to the high correlation between Niño3 and Niño4 (overlapping between the shading and contours). The above zonal differences are more distinct based on N_{EP} and N_{CP} indices as expected (Figures 1d–1f). For example, the maximum correlation between zonal wind and N_{EP} locates around 180°–150°W, while the maximum correlation between zonal wind and N_{CP} locates around 150°–160°E.

3.2. Extratropical Predictors in Pacific

Extratropical sea level pressure (SLP) anomalies in the Pacific are also useful precursors (e.g., Ding, Li, & Tseng, 2015; Ding, Li, Tseng, Sun, & Guo, 2015; You & Furtado, 2017). These remote precursors are the additional triggering forcing, on the top of the dominant internal tropical dynamic, that could further suppress or enhance the final ENSO development through the equatorial ocean-atmosphere coupling (H.-C. Chen et al., 2020; Timmermann et al., 2018). Figure 2 shows the correlation maps of SST (shading) and SLP (contours) anomalies

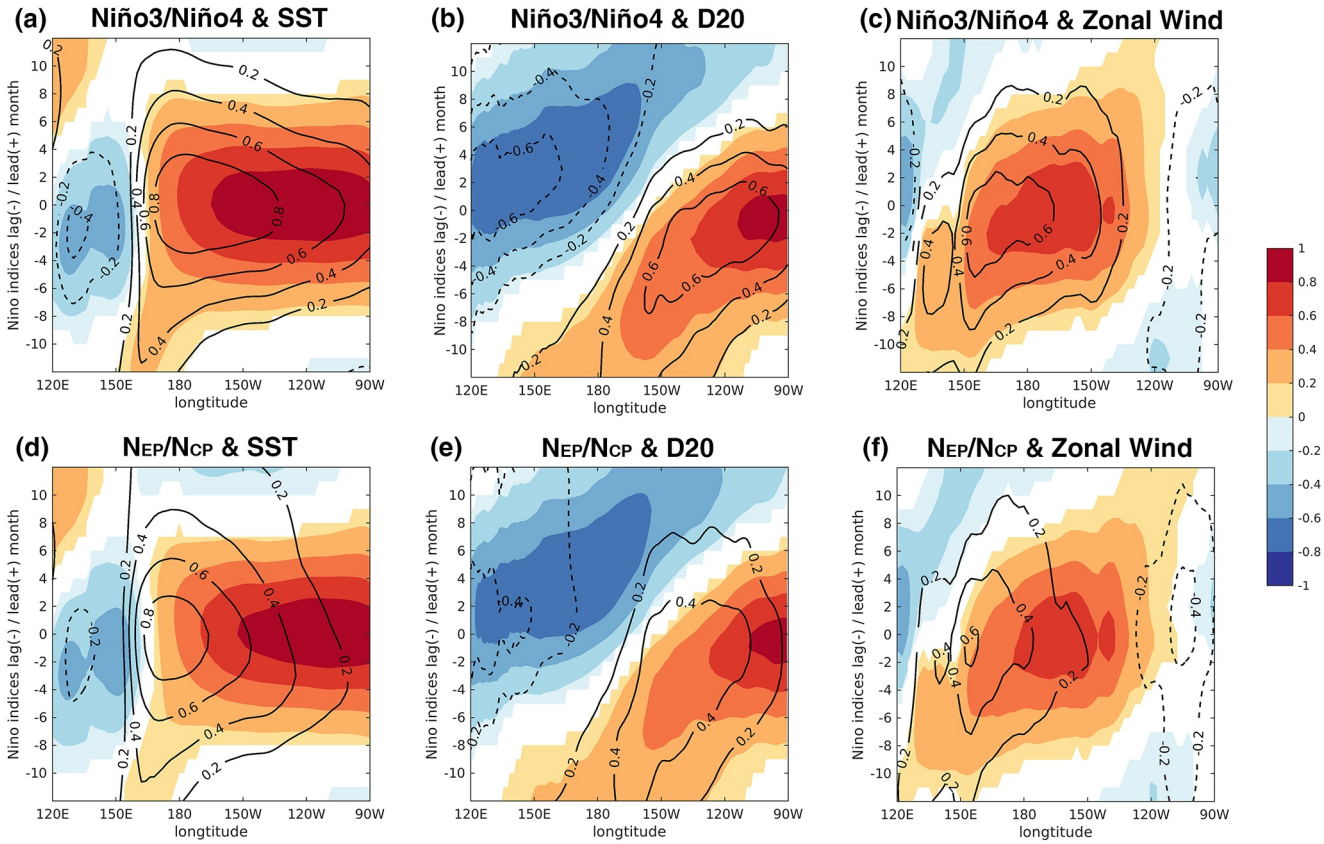

Figure 1. (a) Lead-lag correlations between Niño3 (shading)/Niño4 (contours, positive is solid and negative is dashed) and the 3-month averaged equatorial (5°S–5°N) mean sea surface temperature anomaly (SSTA) during 1980–2020. Shading and contours are all significant at 90% confidence level. Lead times with negative values indicate that the SSTA is leading. (b and c) are the same as (a) but for D20 and zonal wind, respectively. (d–f) are the same as (a–c) but for N_{EP} (shading)/N_{CP} (contours).

at different lead months with boreal winter (December-February) ENSO indices. At the 12-month lead, Niño4 index has more clear extratropical precursors signals than Niño3 index (Figures 2a and 2d), and these signals are strongest at the 9-month lead for both Niño3 and Niño4 indices (Figures 2b and 2e), consistent with those used in H.-C. Chen et al. (2020). However, it appears these precursors are difficult to distinguish for Niño3 and Niño4 indices, while for N_{EP} and N_{CP}, they are very different (Figures 2h and 2k).

For the SLP precursors at 9-month lead, very strong signals can be found in the southern hemisphere for the N_{EP} (Figure 2h) but in the northern hemisphere for the N_{CP} (Figure 2k). Both N_{EP} and N_{CP} show very strong warm VM-like precursors in the northern hemisphere and can directly link to the North Pacific Oscillation (NPO)/Victoria Mode (VM) coupled processes discussed earlier (Ding, Li, Tseng, Sun, & Guo, 2015; Tseng, Ding, & Huang, 2017). The spring VM is caused by the winter NPO which is represented as the second dominant mode of SLP anomalies (Linkin & Nigam, 2008; Rogers, 1981). The following impacts of VM on triggering of ENSO involve the physical process of "seasonal footprinting mechanism" (Vimont et al., 2003) which can further weaken subtropical trade winds, decrease upward latent heat flux and subsequently generate positive tropical SSTAs in the tropical Pacific to weaken zonal SST gradient and also cause strong anomalous westerlies near the equator.

Although the positive SSTAs are not evident in the southern hemisphere for the N_{EP} compared to the N_{CP} at 9-month lead, the southern Pacific quadrapole SST pattern is clear, where the negative anomalies emerge at western tropical Pacific and extend eastward into extratropical regions as two bands. These extratropical quadrapole SST and accompanying SLP patterns can affect ENSO development through ocean-atmosphere interaction (Ding, Li, & Tseng, 2015; You & Furtado, 2017). Through modulation of the climatological southeasterly trade winds, the corresponding South Pacific extratropical signals promote anomalous equatorward ocean mass transport in the eastern equatorial Pacific, facilitating the growth of warm SSTA there and thus promoting EP ENSO events.

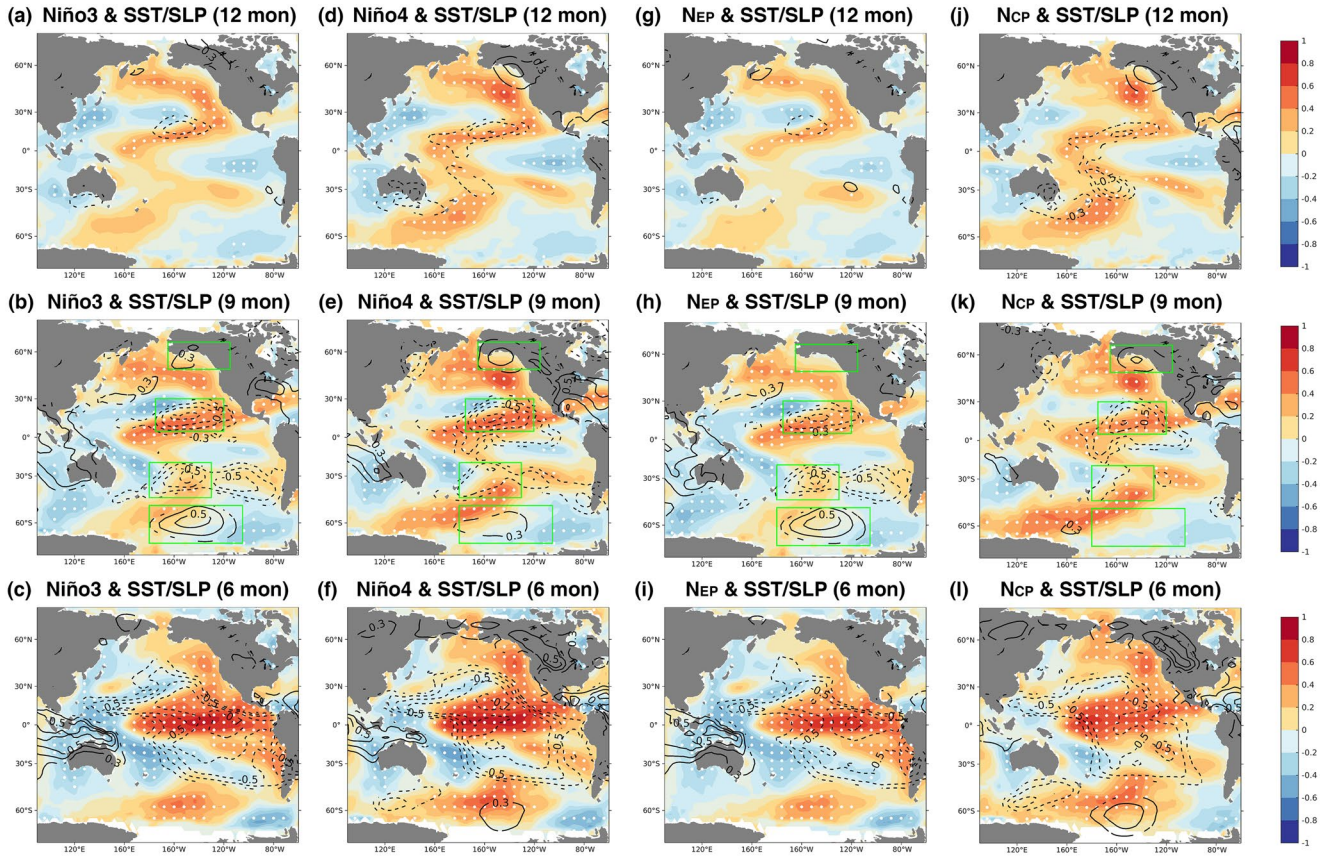

Figure 2. (a) Correlation map of sea surface temperature (SST) (shading) and sea level pressure (SLP) (contours) anomalies at different lead time (12, 9, and 6 month lead from top to bottom, respectively) with boreal winter (December-February) Niño3 index. White dots indicate the correlation of SSTAs exceeding a 90% confidence level using a *t*-test. The SLP anomalies with correlations significant above the 90% confidence level are also shown. The four green boxes (from top to bottom: 165°–115°W, 50°–65°N and 175°–120°W, 5°–30°N and 180°–130°W, 20°–45°S and 180°–105°W, 50°–70°S) are used to define the extratropical precursor index.

For N_{EP} at 6-month lead (Figure 2i), the tropical zonal SSTA dipole gets stronger with typical Southern Oscillation SLP anomalies pattern (positive/negative above the warm pool/eastern Pacific). At this time, no clear positive SLP anomalies can be found in N_{CP} because the SSTA center locates at the central Pacific (Figure 2l). The distinct differences between the two types of ENSO can also be found in the same correlation maps of subsurface D20 and zonal wind anomalies with different ENSO indices (Figure S2 in Supporting Information S1), particularly the locations of large D20 and zonal wind anomalies. Figure 2 clearly shows the key role of extratropical forcing beyond 6-month lead before Bjerknes feedback starts to dominate the development of a matured ENSO in the tropic Pacific. Since these precursors resemble the meridional dipole oscillation from both hemispheres, we select the Northern/Southern Hemisphere SLP dipole precursors (NH/SH, green boxes in Figure 2) to represent the impacts from different hemispheres.

3.3. Predictability

To obtain a deeper understanding of the roles of hemispheric extratropical precursors to clarify their influences on the ENSO predictability, the all-month correlation skill of the ENSO indices predicted by EPMs using different precursors during the period of 1980–2020 are shown in Figure 3. Here, four EPMs based on different predictors are investigated: (a) tropical predictors only, including EP_{SST}, $EP_{WWV}(t)$, and EP_{OA} (EPM_{TD}); (b) tropical and North Pacific extratropical predictors (EPM_{TD+NH}); (c) tropical and South Pacific extratropical predictors (EPM_{TD+SH}); (d) tropical and extratropical predictors, both NH and SH (EPM_{TD+EX}). Compared with the persistence forecast (dashed line on Figure 3), including only the tropical predictors (EPM_{TD}) can greatly enhance the correlation skill for both types of ENSO forecast (Tseng, Hu, et al., 2017). However, the EPM_{TD} prediction features a gradual decline with increasing lead months, particularly for EP type of ENSO (Figures 3a and 3c).

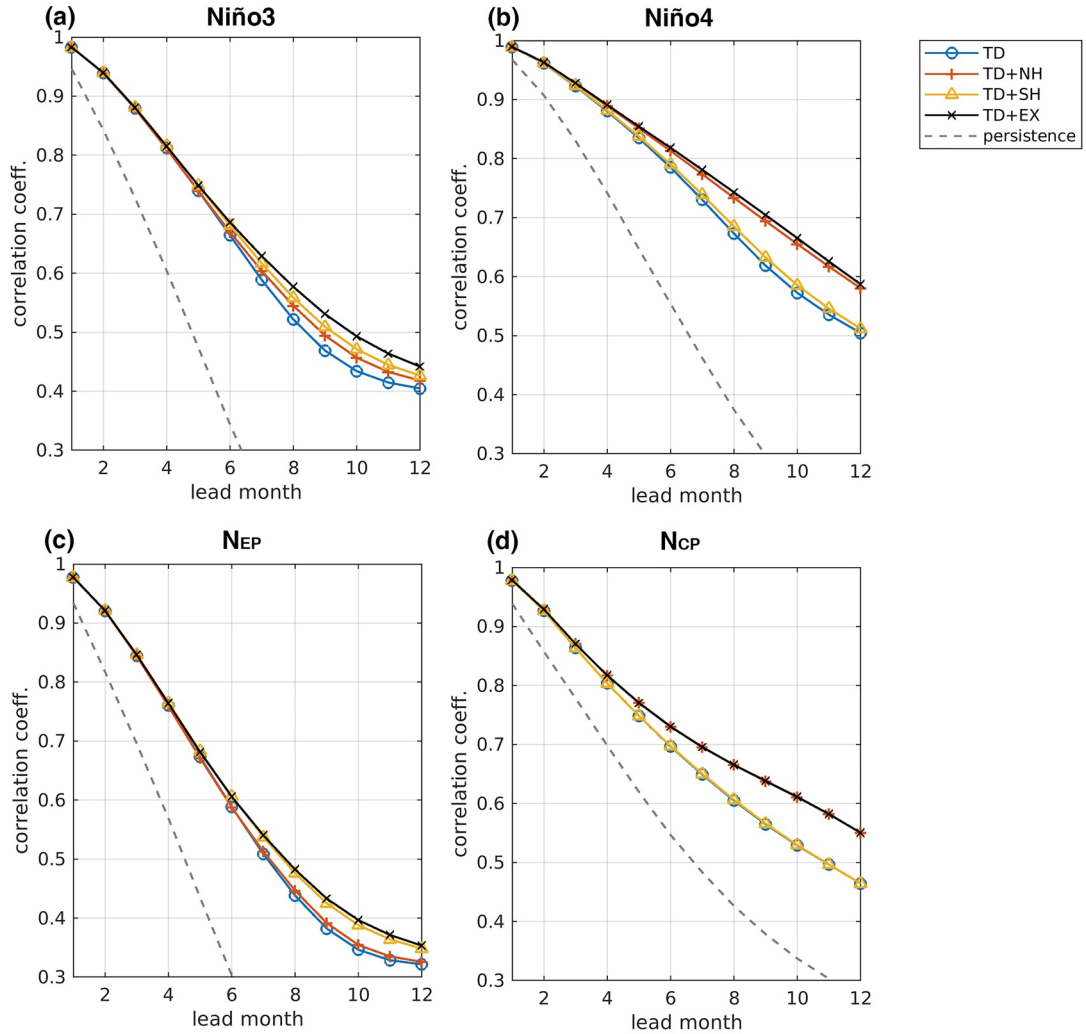

Figure 3. (a) Correlation skill scores (solid lines with markers) of the Niño3 index predicted by different forecast models during the period of 1980–2020. The blue, red, yellow, and black lines indicate EPMs based on tropical predictors only (EPM_{TD}), tropical and North Pacific extratropical predictors (EPM_{TD+NH}), tropical and South Pacific extratropical predictors (EPM_{TD+SH}), and tropical and both Northern Hemisphere (NH) and Southern Hemisphere (SH) extratropical predictors (EPM_{TD+EX}). The persistence forecast is also shown for comparison (dashed line). (b–d) are the same as (a) but for the Niño4, N_{EP}, and N_{CP} indices, respectively.

Consistent with Ren et al. (2019), both N_{EP} and N_{CP} show relatively lower skills compared to Niño3 and Niño4 indices, respectively, due to the spatial complexity of ENSO for N_{EP} and N_{CP} (Timmermann et al., 2018), respectively. According to the typical Recharge Oscillator framework (Jin, 1997), the system has only two degrees of freedom (SST and thermocline anomalies) for Niño3 and Niño4 indices (considering only SST anomalies), however, the system may include more than three degrees of freedom (further considering the spatial structure) for N_{EP} and N_{CP} (Geng et al., 2020). The reduction of ENSO prediction skill is not surprising due to the additional degrees of freedom. We also note that the improvement of N_{EP} compared to the persistent forecast is superior to the improvement of N_{CP}, similar to many previous studies (e.g., Ren et al., 2016, 2019; Zhu et al., 2015). Further including the extratropical SH (NH) precursor can significantly enhance the predictability of N_{EP} (N_{CP}) beyond 6 months as shown in Figure 3c (Figure 3d). These results show that the SH/NH extratropical precursor, respectively, links to the evolution of N_{EP}/N_{CP}. Particularly, there is no further improvement when both SH and NH extratropical precursors (EPM_{TD+EX}) are considered (black crossed lines overlay the yellow triangle and the red plus lines in Figures 3c and 3d, respectively), suggesting the individual (independent) role from the south and North Pacific.

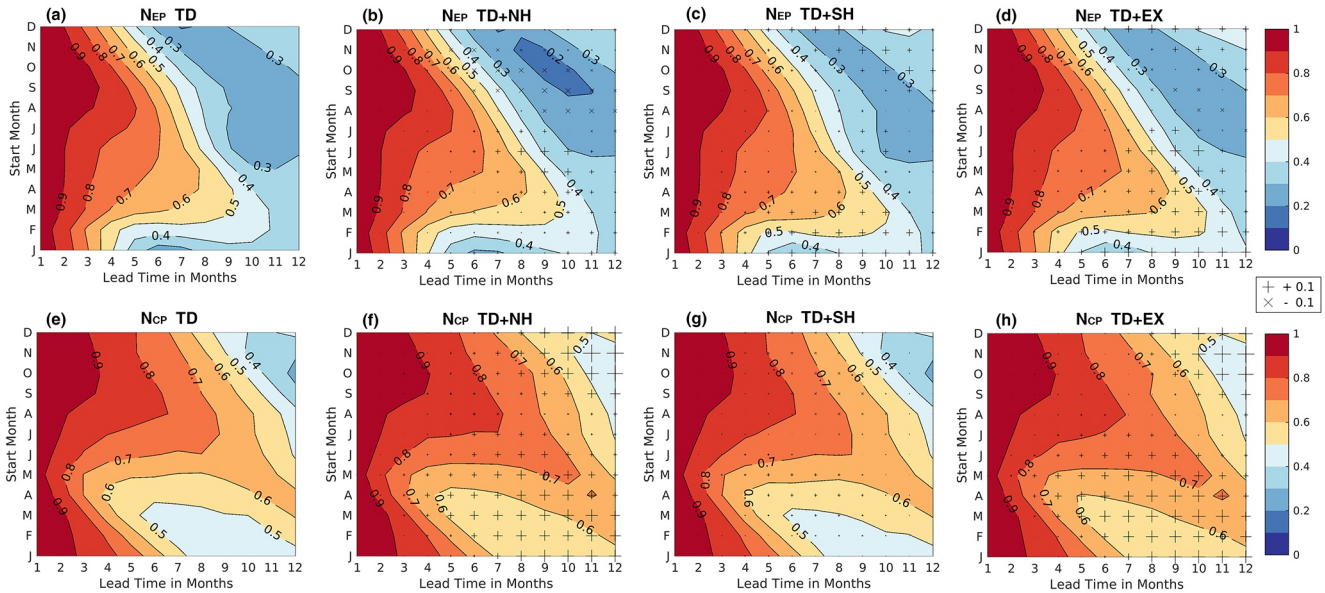

Figure 4. Correlation skill scores (shading) as a function of start calendar month and lead month for the N_{EP} predicted by the (a) TD-only predictor, (b) TD+NH predictor, (c) TD+SH predictor, and (d) TD+EX predictor. In (b–d), the differences relative to the TD-only predictor are denoted by the plus (improved) and cross (deteriorated) symbols (scaled by the symbol size), respectively. (e–h) are the same as (a–d) but for N_{CP}.

We further examine the correlation skill scores as a function of the start calendar month and lead month for the ENSO indices predicted by different predictors (Figure 4). Since N_{EP} and N_{CP} are the better indices for separating the characteristics of EP and CP-ENSO compared to Niño3 and Niño4, only predictions based on N_{EP} and N_{CP} are examined here (similar results are still hold for Niño3 and Niño4 indices, Figure S3 in Supporting Information S1). The baseline model is the EPM_{TD}, which can already provide reasonable forecast while the additional SH and NH precursors and their combination are further included. The SPB, a sudden reduction of the prediction skill in the boreal spring (Webster & Yang, 1992), still exists regardless of the types of ENSO (Figures 4a and 4e).

However, by including the NH extratropical information, the forecast skill for the CP-ENSO (N_{CP}) is greatly enhanced when the start month is before boreal spring (plus symbols during FMA start month with 6–12 months lead in Figure 4f), consistent with the potential impacts of boreal winter NPO on ENSO development discussed extensively (e.g., Ding, Li, Tseng, Sun, & Guo, 2015; Tseng, Ding, & Huang, 2017; Tseng et al., 2020). This also supports the fact that CP-ENSO is directly linked with the NH pathway described in Tseng, Ding, & Huang (2017). For EP-ENSO (N_{EP}), the additional SH precursor can also increase the ENSO prediction skill beyond the SPB (plus symbols during FMA start month with 6–10 month lead in Figure 4c), indicating the impacts of South Pacific extratropical forcing on EP-ENSO. The quadrapole SSTA pattern in the extratropical South Pacific (Figure 2h) triggered by the Pacific–South American (PSA) pattern has an additional influence on EP-ENSO via ocean-atmosphere coupled process (Ding, Li, & Tseng, 2015). But the improvement is not as great as that of the CP-ENSO (measured by the size of plus symbols), suggesting the associated processes may be weaker.

From the above, it is clear that the individual extratropical NH (or SH) precursor can significantly enhance the predictability of CP (or EP)-ENSO for the lead time longer than 6-month, especially beyond the time scale of SPB. The coefficients of the multivariate linear regression model further confirm the relative contributions of each predictor (Figure S4 in Supporting Information S1). Both extratropical predictors (EX_{SH} and EX_{NH}) have increased contributions for the long lead month, indicating the increasing impacts of extratropical influence on the ENSO forecast skill at long lead-month. For the shorter lead-month than 6-month, the SST persistence mainly contributes to the high forecast skill.

We note that adding the NH extratropical forcing has limited contribution to improving the forecast skill of EP-ENSO (slightly improves for the boreal spring-started prediction, Figure 4b) while almost no improvement is achieved for the forecast of CP-ENSO by the inclusion of the SH extratropical forcing (Figure 4g). When extratropical predictors are all included to predict the two types of ENSO, the prediction of N_{CP} has a higher correlation

skill for most of the target and lead months (Figure 4h), except the start months of September–November beyond 10-month lead. Although the correlation skill has been significantly improved by adding the NH precursor, it is still lower than 0.5. The predictions of N_{EP} are less skillful for some of the target and lead months (Figure 4d). In general, these results lend a strong support to clarify the distinct role of SH (NH) extratropical precursor on the EP (CP)-ENSO development from the almost independent predictability viewpoint.

Since 2000, CP-ENSO events have become more frequent than EP-ENSO events, resulting in poor skills in predicting the ENSO after one season (Barnston et al., 2011). The shortening of lead time between WWV and ENSO variability after 2000, suggests the changes of ENSO dynamics based on the Recharge Oscillator framework (Hu et al., 2017). This directly links to the westward shift of the Bjerknes feedback region in the tropical Pacific. The westward shift of the air-sea coupling region corresponds to the reduced zonal advection feedback which increases the ENSO frequency and reduces the growth of coupled instability. Our results also confirmed that the prediction skill of the N_{EP} is much lower for the period 2000–2020 than 1980–1999 (N_{EP}; Figure S5c in Supporting Information S1) due to the change of ENSO dynamics. When the extratropical precursors are further considered, the prediction skill can be significantly improved after 2000 but not before 2000, suggesting the increased impact of extratropical forcing in the first decade of the 21st century (Hu et al., 2017). In contrast, the prediction skills in N_{CP} do not change much before and after 2000 (N_{CP}; Figure S5d in Supporting Information S1). When the information of extratropical precursors is included in the EPM, there is a significant increase in predictive skills for both 1980–1999 and 2000–2020. These differences also indicate that the development of CP-ENSO is highly correlated with extratropical atmospheric forcing associated with the VM evolution in agreement with the literature (reviewed in Yu et al., 2017) and suggest the increasing role of VM on the CP-ENSO dynamics in the recent two decades and future climate change scenario (e.g., Jia et al., 2021).

4. Summary and Discussion

An updated statistical prediction model is used to clarify the distinct impacts of extratropical precursors on the ENSO prediction. This study suggests that adding NH/SH extratropical precursors on a "tropical predictors only" model can enhance the predictability of CP/EP-ENSO, respectively. Particularly, the significant improvement is beyond 6–8 month lead-time (time scale of SPB), consistent with that found in H.-C. Chen et al. (2020). Including NH extratropical precursors effectively increases the predictability of N_{CP} (but no big change on N_{EP}) through the ocean-atmosphere interaction associated with VM, which behaves superior to the limited contribution of NPO on ENSO prediction suggested in Ren et al. (2019). This is possibly due to the difference of baseline model and a shift of definition region in associated with different seasonal impacts of NPO. The forecast skills for the two types of ENSO in our baseline model (EPM_{TD}) perform similar to those shown in Ren et al. (2019), showing a large prediction improvement of N_{EP} compared with the persistence forecast. However, the persistence forecast skill is still much higher for N_{CP} and the extratropical predictors can enhance both types of ENSO resulting from the different hemispheres, leading to an overall high prediction skill for both types of ENSO. Furthermore, Tseng et al. (2020) confirmed that the southern lobe of NPO, particularly its southern tip, was more connected to the ENSO development through the spring VM pattern (or called Pacific Meridional Mode, PMM) than the northern lobe of NPO. Therefore, the late winter to spring NH SLP anomalies associated the NPO/VM evolution plays a more important role in triggering the CP-ENSO (comparing Figure 2j with Figure 2k) rather than the winter NPO pattern used in Ren et al. (2019). Our results confirm CP-ENSO can be enhanced by the North Pacific extratropical forcing suggested in Hu et al. (2017).

Including SH extratropical precursors also enhances the predictability of N_{EP} moderately (but no big change on N_{CP}). You and Furtado (2017) suggested that the southern Pacific SLP changes may weaken the southeasterly trade winds and promote the charging of the eastern equatorial Pacific WWV through the Subtropical Cell transport due to the wind stress curl change (Figure S2i in Supporting Information S1), consistent with H.-C. Chen et al. (2015). They further suggested that the SH precursors can be a reliable predictor for the type of ENSO events at 3–6 month lead. Their results supported the dynamical processes discussed above for the enhanced predictability found here (their Figure 2). We further clarify that the SH extratropical signals can also lead to the improvement of N_{EP} prediction beyond 6-month lead. It is very clear that the signatures of WWV differ greatly between the two types of ENSO events (comparing Figures S2i and S2l in Supporting Information S1) more than 6-month earlier, suggesting the charging role of equatorial Pacific.

Finally, the predictability of CP indices does not significantly decrease after 2000, while the predictability of EP indices drops dramatically, suggesting the strengthening impact of Victoria Mode on the CP-ENSO in the recent two decades. These decadal changes also support the physical interpretation of the distinct hemispheric contributions addressed here. Our results suggest that CP-ENSO can be more predictable than the EP-ENSO as long as the extratropical predictors are appropriately included. These results also support the possible triggering of EP- and CP-ENSO through their hemispheric evolutions from the viewpoint of predictability.

Data Availability Statement

All datasets used in this research can be accessed via the following websites: ERSSTv5 at https://psl.noaa.gov/data/gridded/data.noaa.ersst.v5.html; GODAS at https://cfs.ncep.noaa.gov/cfs/godas/pentad/; NCEP-NCAR Reanalysis at https://psl.noaa.gov/data/gridded/data.ncep.reanalysis.surface.html. Forecasted data in this research can be obtained from the table (NTU CODA) at https://iri.columbia.edu/our-expertise/climate/forecasts/enso/current/?enso_tab=enso-sst_table.

Acknowledgments
Constructive comments from two anonymous reviewers are appreciated. Y.-H. Tseng and J.-H. Huang acknowledge the support of the MOST Grants 107-2611-M-002-013-MY4 and 108-2111-M-002-006-MY3, Taiwan.

References

Ashok, K., Behera, S. K., Rao, S. A., Weng, H., & Yamagata, T. (2007). El Niño Modoki and its possible teleconnection. *Journal of Geophysical Research*, *112*(C11).

Barnston, A. G., Tippett, M. K., L'Heureux, M. L., Li, S., & DeWitt, D. G. (2011). Skill of real-time seasonal ENSO model predictions during 2002–11: Is our capability increasing? *Bulletin of the American Meteorological Society*, *93*(5), 631–651. https://doi.org/10.1175/BAMS-D-11-00111.1

Behringer, D. W., & Xue, Y. (2004). Evaluation of the global ocean data assimilation system at NCEP: The Pacific Ocean. In *Proceedings of eighth symposium on integrated observing and assimilation systems for atmosphere, oceans, and land surface* (pp. 11–15).

Chen, C., Cane, M. A., Wittenberg, A. T., & Chen, D. (2017). ENSO in the CMIP5 simulations: Life cycles, diversity, and responses to climate change. *Journal of Climate*, *30*(2), 775–801.

Chen, H.-C., Sui, C. H., Tseng, Y. H., & Huang, B. (2015). An analysis of the linkage of pacific subtropical cells with the recharge-discharge processes in ENSO evolution. *Journal of Climate*, *28*(9), 3786–3805. https://doi.org/10.1175/JCLI-D-14-00134.1

Chen, H.-C., Tseng, Y. H., Hu, Z. Z., & Ding, R. (2020). Enhancing the ENSO predictability beyond the spring barrier. *Scientific Reports*, *10*(1), 1–12. https://doi.org/10.1038/S51598-020-57853-7

Ding, R., Li, J., & Tseng, Y. (2015). The impact of South Pacific extratropical forcing on ENSO and comparisons with the North Pacific. *Climate Dynamics*, *44*(7), 2017–2034. https://doi.org/10.1007/s00382-014-2303-5

Ding, R., Li, J., Tseng, Y. H., Sun, C., & Guo, Y. (2015). The Victoria mode in the North Pacific linking extratropical sea level pressure variations to ENSO. *Journal of Geophysical Research: Atmospheres*, *120*(1), 27–45. https://doi.org/10.1002/2014JD022221

Geng, T., Cai, W., & Wu, L. (2020). Two types of ENSO varying in tandem facilitated by nonlinear atmospheric convection. *Geophysical Research Letters*, *47*(15), e2020GL088784.

Hendon, H. H., Lim, E., Wang, G., Alves, O., & Hudson, D. (2009). Prospects for predicting two flavors of El Niño. *Geophysical Research Letters*, *36*(19). https://doi.org/10.1029/2009GL040100

Hu, Z. Z., Humar, A., Zhu, J., Huang, B., Tseng, Y. H., & Wang, X. (2017). On the shortening of the lead time of ocean warm water volume to ENSO SST since 2000. *Scientific Reports*, *7*, 4294.

Huang, B., Thorne, P. W., Banzon, V. F., Boyer, T., Chepurin, G., Lawrimore, J. H., et al. (2017). Extended reconstructed sea surface temperature, version 5 (ERSSTv5): Upgrades, validations, and intercomparisons. *Journal of Climate*, *30*(20), 8179–8205.

Jia, F., Cai, W., Gan, B., Wu, L., & Di Lorenzo, E. (2021). Enhanced North pacific impact on El Niño/southern oscillation under greenhouse warming. *Nature Climate Change*, *11*(10), 840–847.

Jin, F. F. (1997). An equatorial ocean recharge paradigm for ENSO. Part I: Conceptual model. *Journal of the Atmospheric Sciences*, *54*(7), 811–829.

Kalnay, E., Kanamitsu, M., Kistler, R., Collins, W., Deaven, D., Gandin, L., et al. (1996). The NCEP/NCAR 40-year reanalysis project. *Bulletin of the American Meteorological Society*, *77*(3), 437–472.

Kao, H. Y., & Yu, J. Y. (2009). Contrasting eastern-Pacific and central-Pacific types of ENSO. *Journal of Climate*, *22*(3), 615–632. https://doi.org/10.1175/2008JCLI2309.1

Kim, H. M., Webster, P. J., & Curry, J. A. (2009). Impact of shifting patterns of Pacific Ocean warming on North Atlantic tropical cyclones. *Science (New York, N.Y.)*, *325*(5936), 77–80. https://doi.org/10.1126/SCIENCE.1174062

Linkin, M. E., & Nigam, S. (2008). The North Pacific Oscillation–west Pacific teleconnection pattern: Mature-phase structure and winter impacts. *Journal of Climate*, *21*(9), 1979–1997.

Meinen, C. S., & McPhaden, M. J. (2000). Observations of warm water volume changes in the equatorial Pacific and their relationship to El Nino and La Nina. *Journal of Climate*, *13*(20), 3551–3559.

Ren, H. L., & Jin, F. F. (2011). Niño indices for two types of ENSO. *Geophysical Research Letters*, *38*(4). https://doi.org/10.1029/2010GL046031

Ren, H. L., & Jin, F. F. (2013). Recharge oscillator mechanisms in two types of ENSO. *Journal of Climate*, *26*(17), 6506–6523.

Ren, H. L., Jin, F. F., Tian, B., & Scaife, A. A. (2016). Distinct persistence barriers in two types of ENSO. *Geophysical Research Letters*, *43*(2010), 10973–10979. https://doi.org/10.1002/2016GL071015

Ren, H. L., Zuo, J., & Deng, Y. (2019). Statistical predictability of Niño indices for two types of ENSO. *Climate Dynamics*, *52*(9–10), 5361–5382. https://doi.org/10.1007/S00382-018-4453-3/FIGURES/12

Rogers, J. C. (1981). The North Pacific oscillation. *Journal of Climatology*, *1*(1), 39–57.

Takahashi, K., Montecinos, A., Goubanova, K., & Dewitte, B. (2011). ENSO regimes: Reinterpreting the canonical and Modoki El Niño. *Geophysical Research Letters*, *38*(10).

Tao, L., Duan, W., & Vannitsem, S. (2020). Improving forecasts of El Niño diversity: A nonlinear forcing singular vector approach. *Climate Dynamics*, *55*(3–4), 739–754. https://doi.org/10.1007/S00382-020-05292-5/TABLES/3

Timmermann, A., An, S.-I., Kug, J.-S., Jin, F.-F., Cai, W., Capotondi, A., et al. (2018). El Niño-southern oscillation complexity. *Nature*, *559*(7715), 535.

Tseng, Y., Hu, Z.-Z., Ding, R., & Chen, H.-C. (2017). An ENSO prediction approach based on ocean conditions and ocean-atmosphere coupling. *Climate Dynamics*, *48*(5), 2025–2044. https://doi.org/10.1007/s00382-016-3188-2

Tseng, Y. H., Ding, R., & Huang, X. M. (2017). The warm Blob in the northeast Pacific: The bridge leading to the 2015/16 El Niño. *Environmental Research Letters*, *12*(5). https://doi.org/10.1088/1748-9326/aa67c3

Tseng, Y. H., Ding, R., Zhao, S., Kuo, Y. C., & Liang, Y. C. (2020). Could the north Pacific oscillation be modified by the initiation of the East Asian winter monsoon? *Journal of Climate*, *33*(6), 2389–2406. https://doi.org/10.1175/JCLI-D-19-0112.1

Vimont, D. J., Wallace, J. M., & Battisti, D. S. (2003). The seasonal footprinting mechanism in the Pacific: Implications for ENSO. *Journal of Climate*, *16*, 2668–2675.

Webster, P. J., & Yang, S. (1992). Monsoon and ENSO: Selectively interactive systems. *Quarterly Journal of the Royal Meteorological Society*, *118*(507), 877–926. https://doi.org/10.1002/QJ.49711850705

Yang, S., & Jiang, X. (2014). Prediction of eastern and central pacific ENSO events and their impacts on East Asian climate by the NCEP climate forecast system. *Journal of Climate*, *27*(12), 4451–4472. https://doi.org/10.1175/JCLI-D-13-00471.1

You, Y., & Furtado, J. C. (2017). The role of South Pacific atmospheric variability in the development of different types of ENSO. *Geophysical Research Letters*, *44*, 7438–7446. https://doi.org/10.1002/2017GL073475

Yu, J. Y., & Fang, S. W. (2018). The distinct contributions of the seasonal footprinting and charged-discharged mechanisms to ENSO complexity. *Geophysical Research Letters*, *45*(13), 6611–6618.

Yu, J.-Y., Wang, X., Yang, S., Paek, H., & Chen, M. (2017). The changing El Niño-southern oscillation and associated climate extremes. In S.-Y. S. Wang, J.-H. Yoon, C. C. Funk, & R. R. Gillies (Eds.), *Geophysical monograph series* (pp. 1–38). John Wiley & Sons, Inc. https://doi.org/10.1002/9781119068020.ch1

Zhu, J., Huang, B., Cash, B., Kinter, J. L., Manganello, J., Barimalala, R., et al. (2015). ENSO prediction in project minerva: Sensitivity to atmospheric horizontal resolution and ensemble size. *Journal of Climate*, *28*(5), 2080–2095. https://doi.org/10.1175/JCLI-D-14-00302.1